Electronic Supplementary Material (ESI) for Dalton Transactions.

Supporting information

Synergistic dual sites of Zn-Mg on hierarchical porous carbon as an advanced oxygen reduction electrocatalyst for Zn–air batteries

Mincong Liu, [a] Jing Zhang, [b] Yan Peng [a] and Shiyou Guan *[a]

a. Department of Chemistry, College of Science, Shanghai University, 99 Shang-Da Road, Shanghai 200444, China; Email: syguan@shu.edu.cn

b. College of Sciences&Institute for Sustainable Energy, Shanghai University, 99 Shang-Da Road, Shanghai 200444, China.

1. Materials characterizations

The morphologies and structures were conducted with scanning electron microscopy (SEM, ZEISS Gemini 300), transmission electron microscopy (TEM, JEOL-2100F) and high-angle annular dark-field scanning transmission electron microscopy (HAADF-STEM) with energy dispersive spectrometry (EDS) (Tecnai G2 F20 electron microscope). X-ray diffraction (XRD) was analyzed by using a Bruker D8 advanced X-ray diffractometer with Cu Kα (40 kV, 40 mA). Raman spectrum was obtained on the Horiba Evolution laser Raman spectrometer (under excitation at 532 nm). X-ray photoelectron spectroscopy (XPS) was measured by using Thermo Scientific K-Alpha spectrometer. Brunauer–Emmett–Teller (BET) specific surface areas was collected nitrogen adsorption–desorption analyses by using an ASAP 2460 instrument at 77 K.

2. Electrochemical measurements

ORR catalytic activity was performed on a CHI760E electrochemical workstation analyzer (Cheng Hua Instruments, Inc., Shanghai, China) with a standard three-electrode system. The reference electrode and the counter electrode are Ag/AgCl electrode and graphite rod, respectively. The catalyst coated glassy carbon (GC, 5.0 mm diameter) electrodes served as the working electrodes. To prepare a homogeneous catalytic ink, 5 mg of the catalyst was mixed with Nafion solution (40 μL), DI water (480 μL) and ethanol (480 μL) using dispersed ultrasonically for 60 min. Then, 10μL catalytic ink was cast onto the glassy carbon disk electrode and dried at room temperature. Cyclic voltammetry (CV) curves were recorded with a sweep rate of 50mV s^{-1} in N_2/O_2-saturated 0.1 M KOH. A series of Linear sweep voltammetry (LSV) tests were performed at rotating speed from 400 to 2025 rpm with a scan rate of 10 mV s^{-1} in O_2-saturated 0.1 M KOH.

The electron transfer number (n) and kinetic current density (J_k) were calculated based on the Koutechy-Levich (K-L) equation:

$$\frac{1}{J}=\frac{1}{J_L}+\frac{1}{J_K}=\frac{1}{J_K}\frac{1}{B\omega^{1/2}}\#(1)$$

$$B=0.2nFC_0D_0^{2/3}\upsilon^{-1/6}\#(2)$$

where J is the measured current density, J_K and J_L are the kinetic and diffusion-limiting current densities, ω is the rotating speed of the disk, F is the Faraday constant (96485 C·mol^{-1}), C_0 is the bulk concentration of O_2 (1.2×10^{-6} mol cm^{-3}), D_0 is the diffusion coefficient of O_2 (1.9 × 10-5cm^2 s^{-1}), and υ is the kinematic viscosity of the electrolyte (0.01 cm^2 s^{-1}).s

The hydrogen peroxide yield (%H_2O_2) and electron transfer number (n) were determined by rotating ring disk electrode (RRDE, Pine) measurements based on the following two equations:

$$H_2O_2(\%) = 200 \times \frac{I_r/N}{I_d + I_r/N} \#(3)$$

$$n = 4 \times \frac{I_d}{I_d + I_r/N} \#(4)$$

where I_d is the disk current, I_r is the ring current, and N=0.37 is the current collection efficiency of the Pt ring.

3. Zn-air battery test

A homemade Zn–air battery was assembled with a Zn/Mg-N-C catalyst-coated carbon paper as the air cathode with a loading density of 0.52 mg cm^{-2}, a Zn plate anode and 6 M KOH + 0.1 M $ZnCl_2$ aqueous electrolyte. The catalyst ink includes 5 mg of catalyst, 5 mg of RuO_2, containing 40 µL of Nafion, 480 µL of DI water and 480 µL ethanol. The ZABs equipped with Pt/C was also fabricated and measured under the same conditions for comparison for comparison.

4. Theoretical calculation

The first principle calculations are performed by Vienna Ab initio Simulation Package(VASP)[1] with the projector augmented wave (PAW) method[2]. The exchange-functional is treated using the Perdew-Burke-Ernzerhof (PBE)[3] functional, in combination with the DFT-D3 correction[4]. The cut-off energy of the plane-wave basis is set at 450 eV. For the optimization of both geometry and lattice size, the Brillouin zone integration is performed with 2*2*1 Monkhorts-Pack[5] kpoint sampling. The self-consistent calculations apply a convergence energy threshold of 10-5 eV. The equilibrium geometries and lattice constances are optimized with maximum stress on each atom within 0.02 eV/Å.

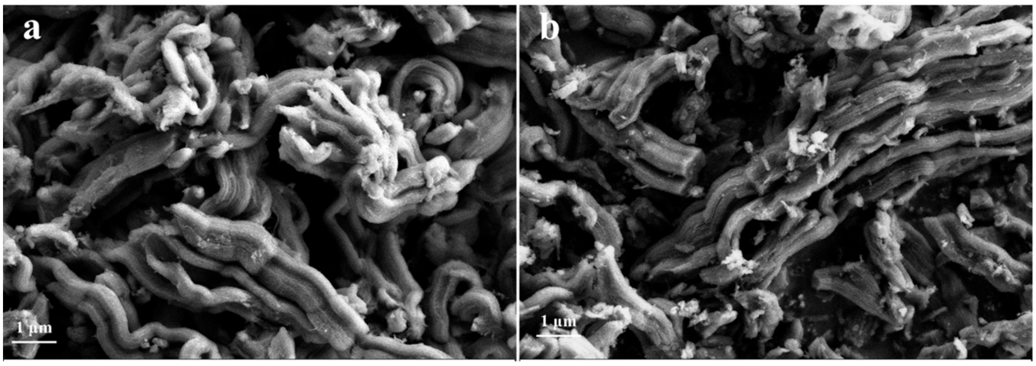

Fig. S1. SEM images of (a) Zn-N-C and (b) Mg-N-C.

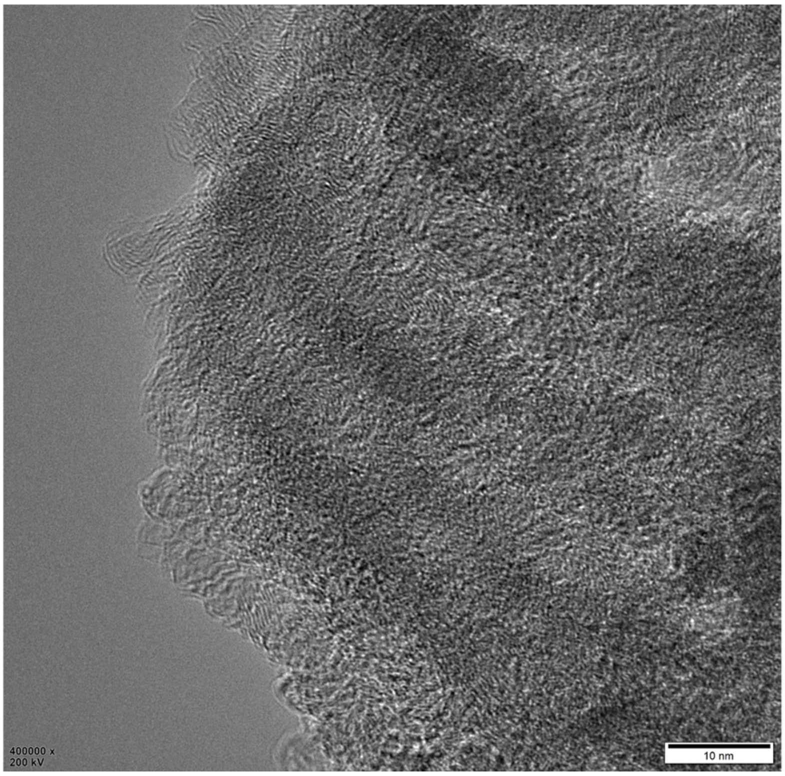

Fig. S2. HRTEM of Zn/Mg-N-C.

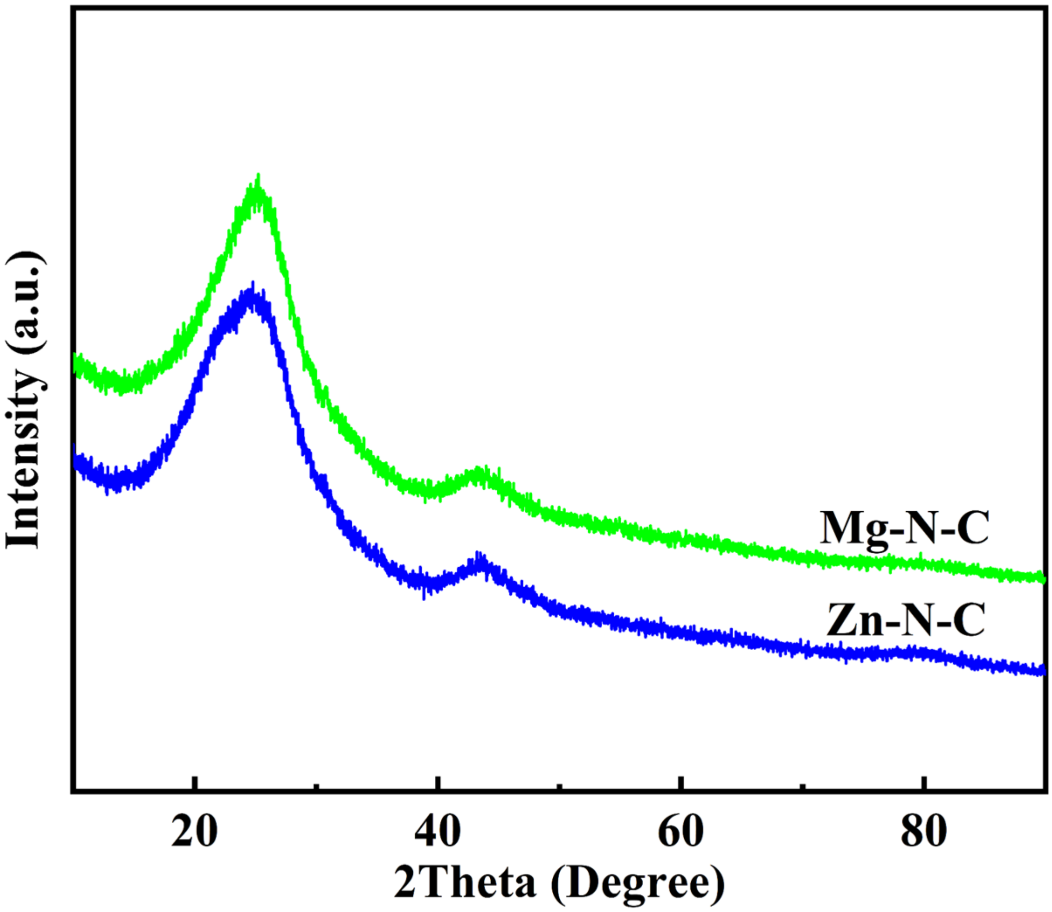

Fig. S3. XRD pattern of Mg-N-C and Zn-N-C.

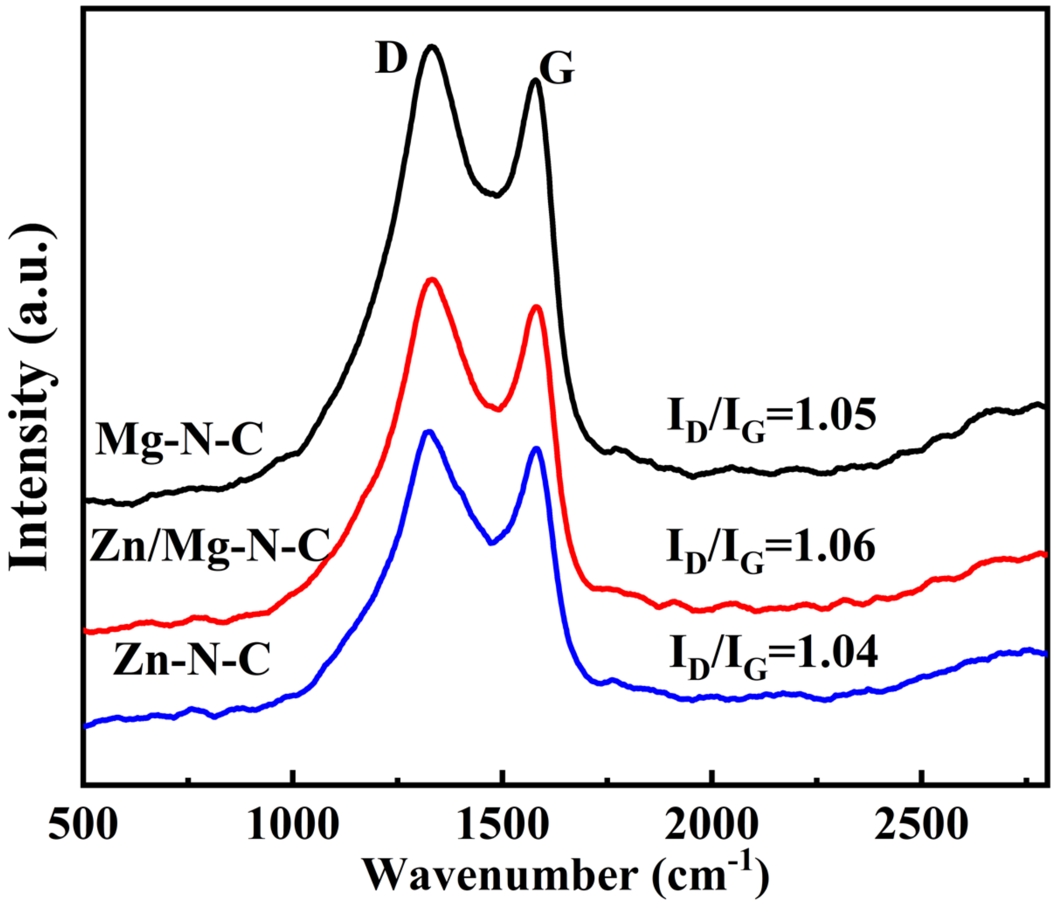

Fig. S4. Raman spectra of Zn/Mg-N-C, Zn-N-C and Mg-N-C.

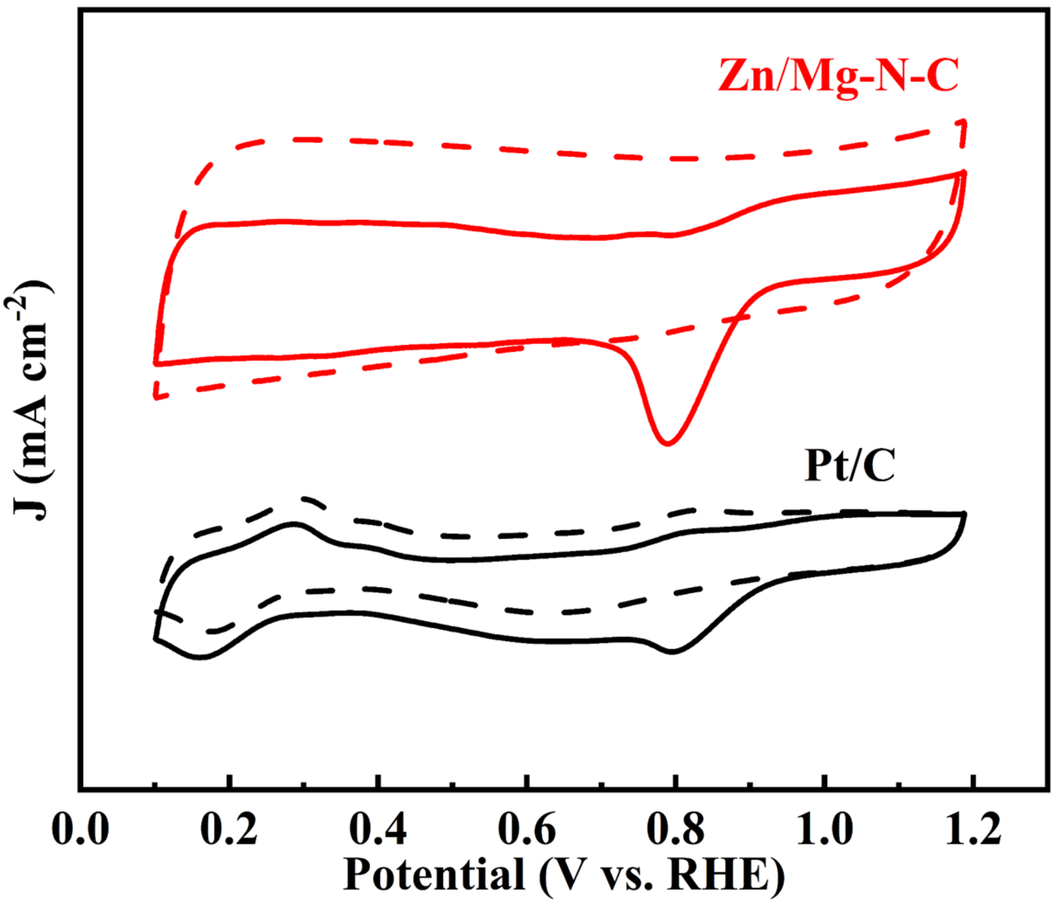

Fig. S5. CV curves for Zn/Mg-N-C, and Pt/C in N_2/O_2-saturated solution at a scan rate of 50 mV s^{-1}.

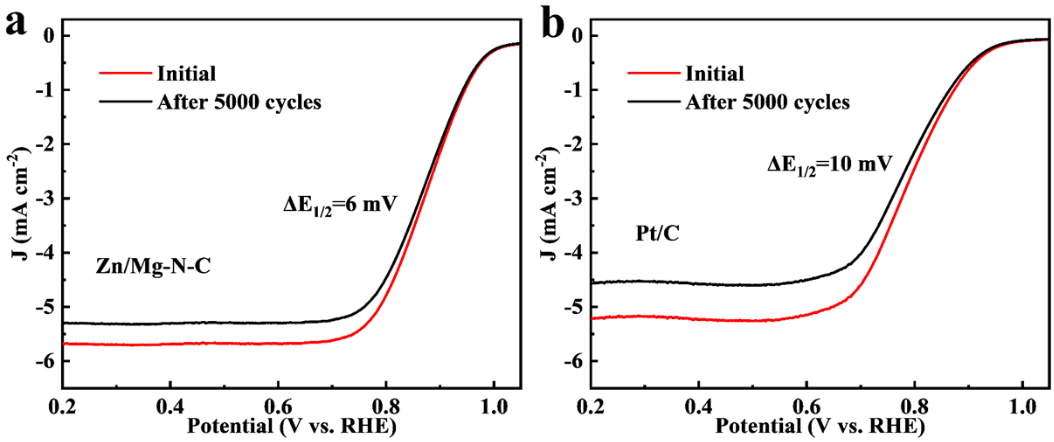

Fig. S6. RDE curves recorded in 0.1 M KOH before and after 5,000 cycles for Zn/Mg-N-C (a) and Pt/C (b).

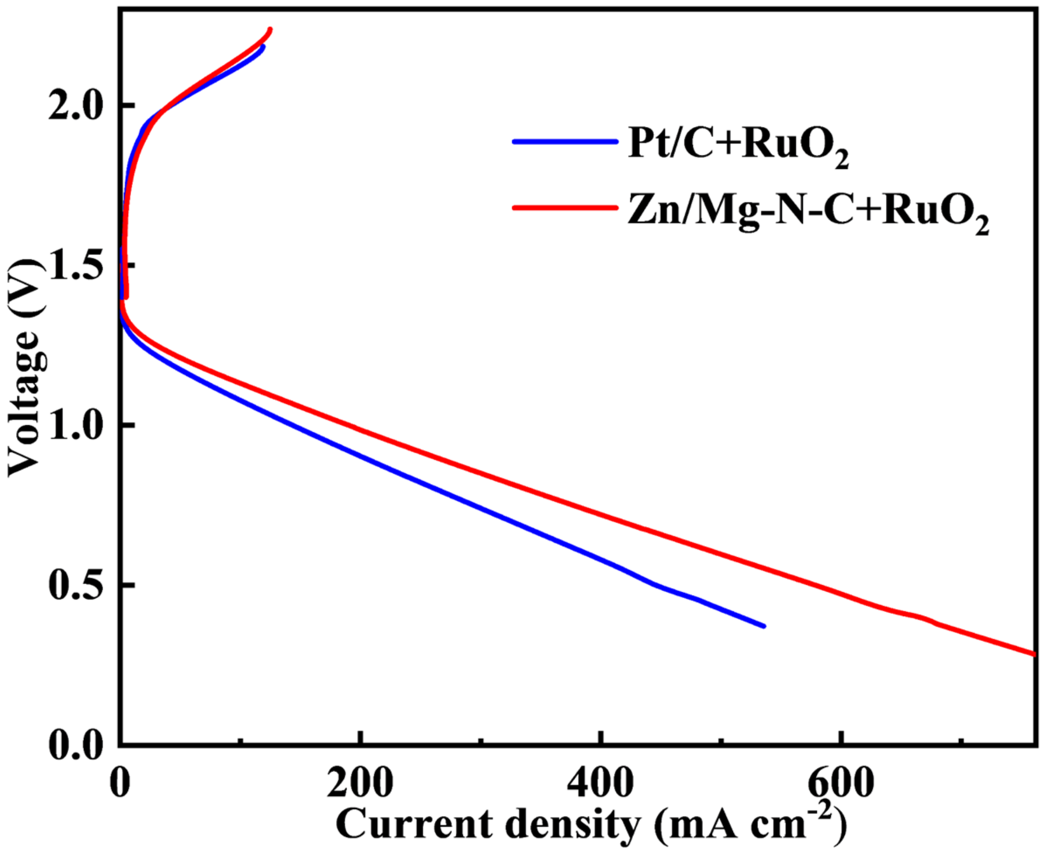

Fig. S7. Discharge and charge polarization curves of Zn/Mg-N-C+RuO_2-based ZABs, and Pt/C+RuO_2-based ZABs for Zn-air battery.

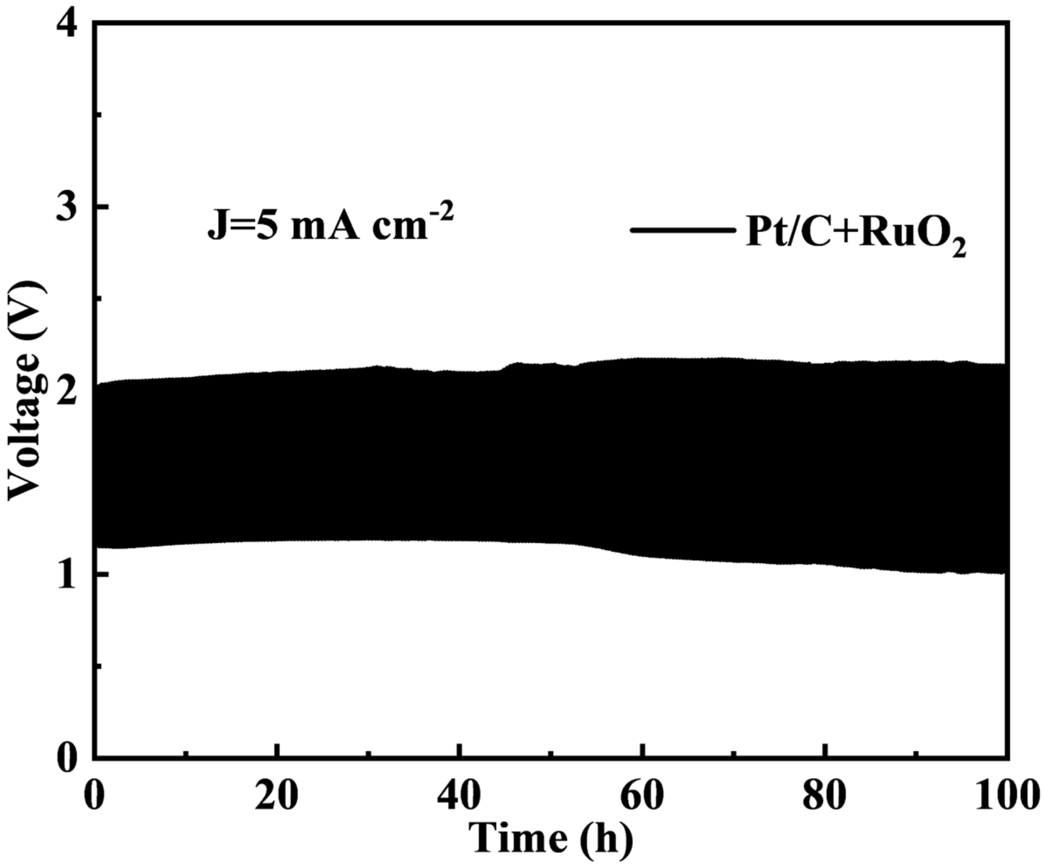

Fig. S8. Cycling tests of batteries for Pt/C+RuO_2-based ZABs at a current density of 5 mA cm^{-2}.

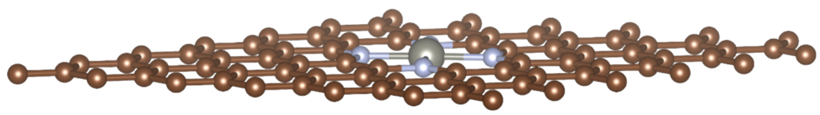

Fig. S9 Optimized geometry of Zn-N-C.

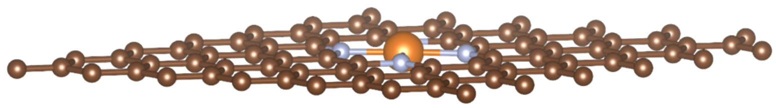

Fig. S10 Optimized geometry of Mg-N-C.

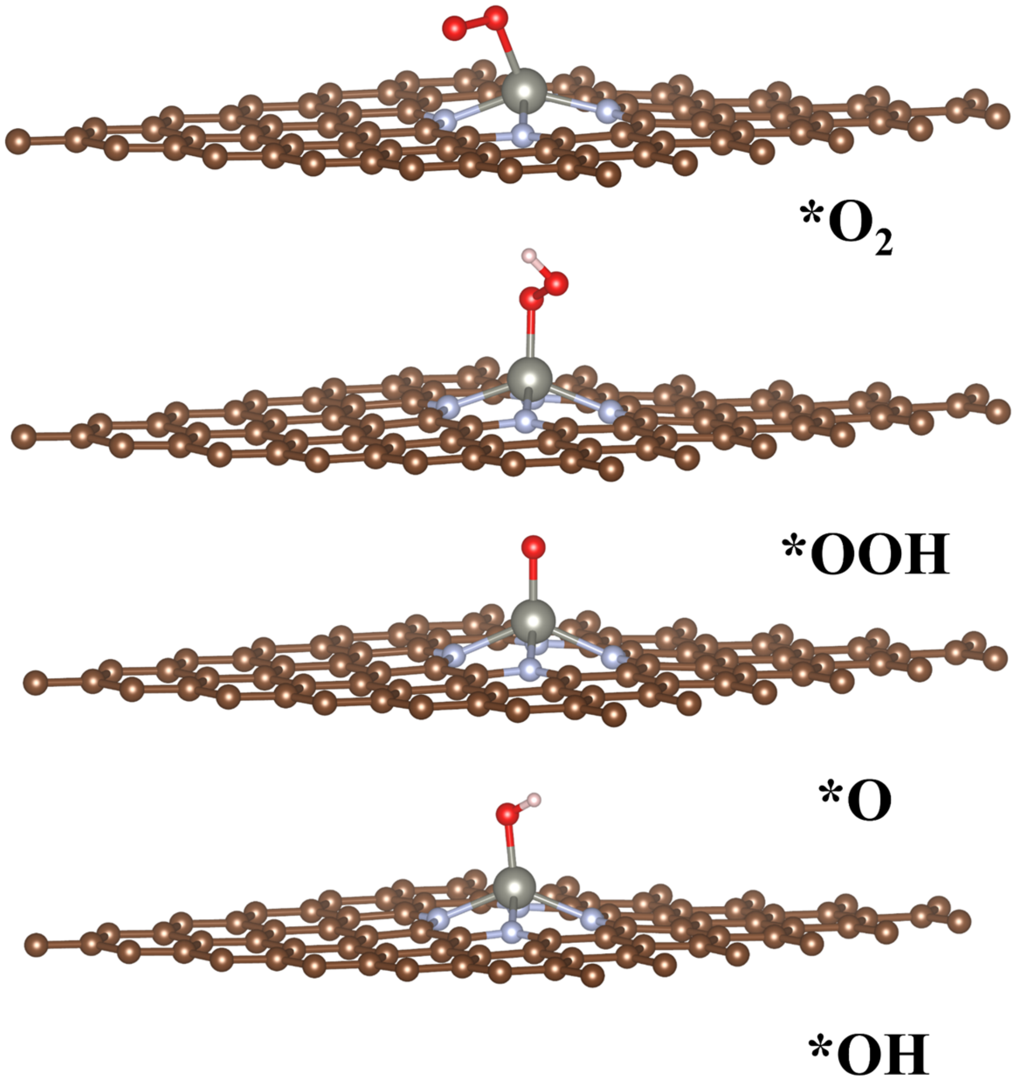

Fig. S11 The models of *O_2, *OOH, *O, *OH intermediate adsorbed on the active site of Zn -N-C.

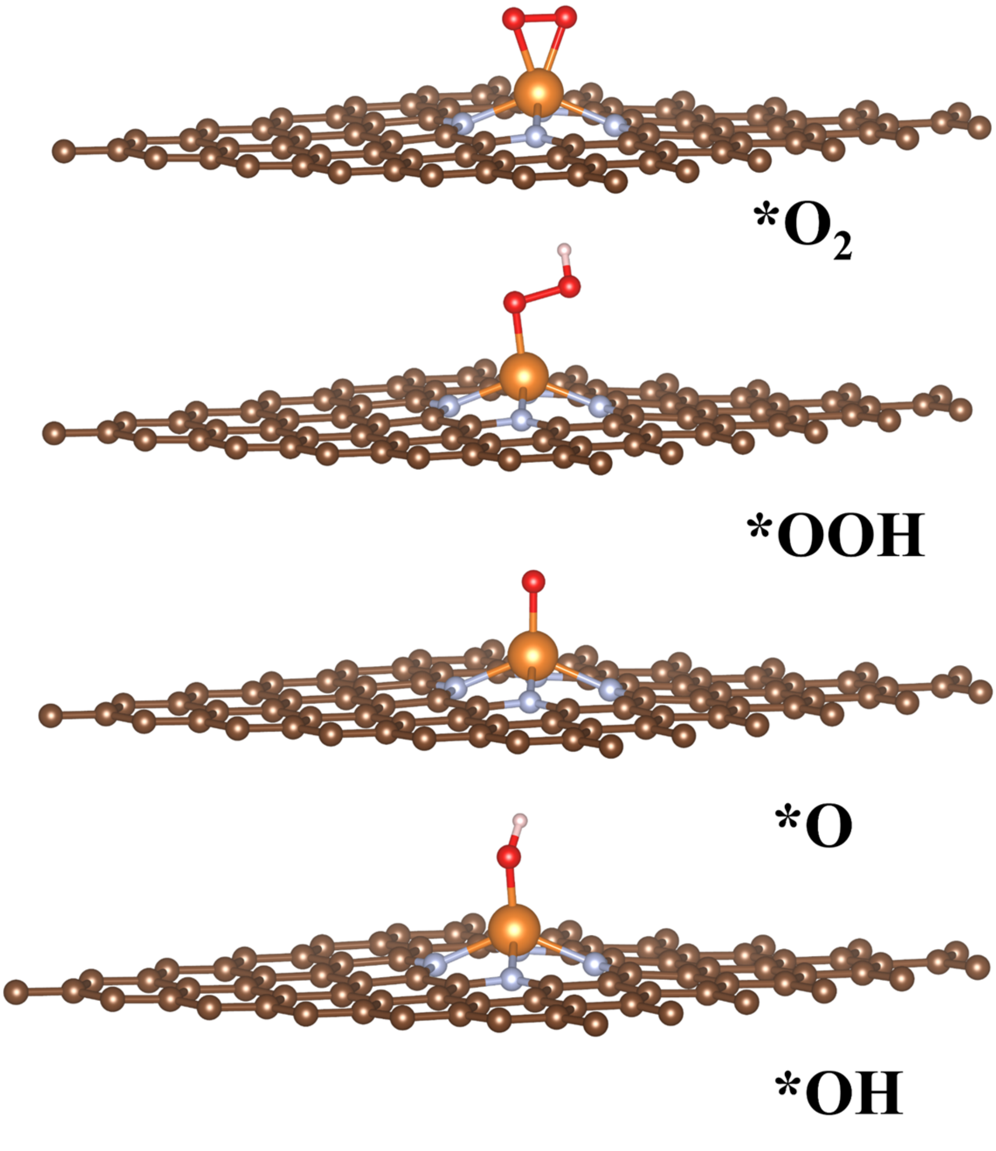

Fig. S12 The models of *O_2, *OOH, *O, *OH intermediate adsorbed on the active site of Mg-N-C.

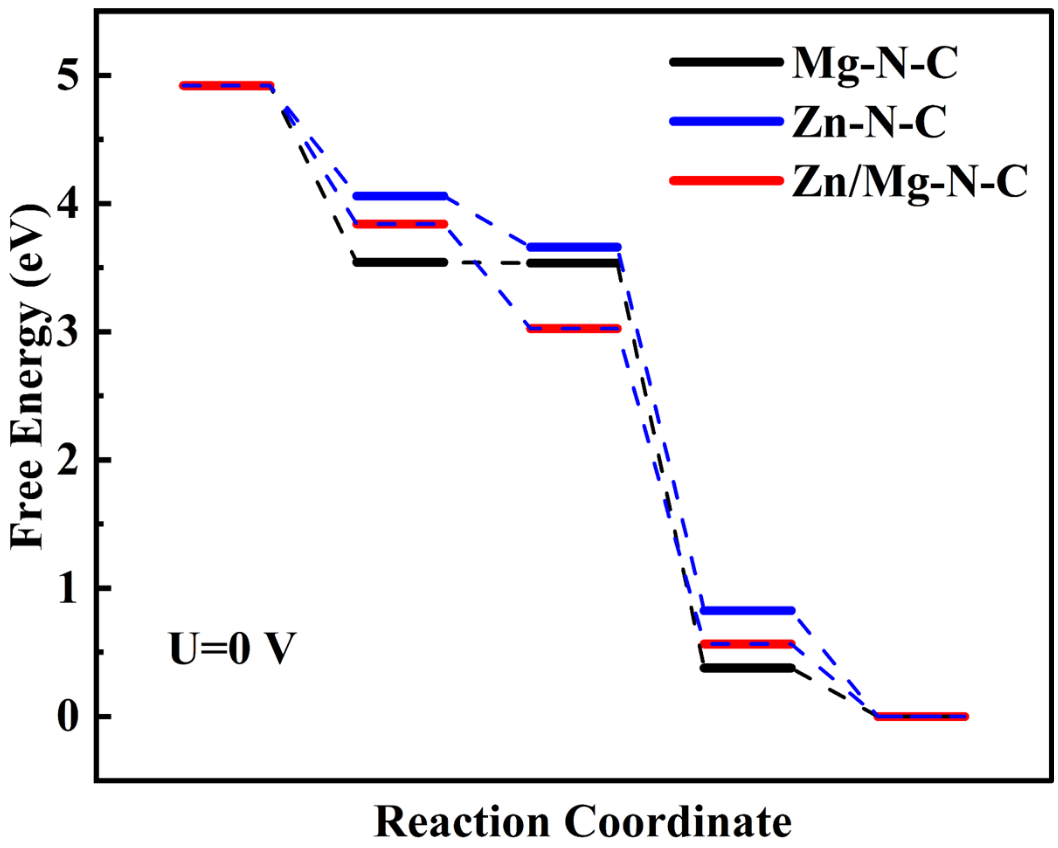

Fig. S13 The Gibbs free energy diagram of the ORR on Zn/Mg-N-C, Zn-N-C and Mg-N-C obtained from DFT calculations (U=0 V).

Table S1. The Content of Zn and Mg in Zn/Mg-N-C

Catalyst	Zn content (wt%)	Mg content (wt%)
Zn/Mg-N-C	0.57	0.21

Table S2. Comparison of electrocatalytic ORR activity as well as ZABs performance of recently reported metal doped carbon-based electrocatalysts

Sample	Half-wave potential (V vs. RHE)	Power dendity (mW cm^{-2})	Ref.
Zn/Mg-N-C	0.89	298.7	This work
Fe/Co NPs	0.82	124.9	Nano-Micro Lett., 2023, 15, 26.
$ZnCo_2$@NCNTs-800	0.85	194.3	Chem. Eng. J., 2022, 429, 132199.
Mg-N-C@800	0.80	N.A.	Appl. Mater. Today, 2020, 21, 100846.
P–Fe–N-CNTs	0.88	145	Appl. Catal., B, 2023, 327, 122469.
NC-Co_3O_4/CC	0.87	82	Adv. Mater., 2017, 29, 1704117.
Zn-N-C	0.873	N.A.	Angew. Chem. 2019, 58, 7035-7039
Fe/SNCFs-NH	0.89	255.84	Adv. Mater., 2022, 34, 2105410.
SSM/Co4N/CoNC	0.83	105	Small, 2022, 18, 2105887.
Fe-NSDC	0.84	225.1	Small, 2019, 15, 1900307.
Cu/Zn-NC	0.83	N.A.	Angew. Chem., 2021, 60, 14005-14012.
Fe–Co DSAC	0.86	152.8	Energy Storage Mater., 2022, 45, 805–813.
Co/CNT_10 Mg/Ni	0.75	181	J. Mater. Chem. A, 2021, 9, 25160–25167.
ZnCo-HNC	0.82	123.7	Small 2022, 18, 2107141
SA Fe@ZrO_2/NC	0.86	250	Chem. Eng. J., 2021, 420, 129938
$ZnCo_2Se_4$@rGO	0.802	137.1	Small 2023, 19, 2207096
Mo2C/MoC/Co@CNTs	0.82	134	J. Power Sources, 2024, 595, 234063
FeSA-N-C	0.89	N.A.	Angew. Chem., 2018, 57, 8525-8529.
ZnSe@PNC	0.905	126	Chem Eng J, 2024, 481, 148598.
Fe/Zn–N–C	0.906	N.A.	Energ Environ Sci, 2022, 15, 1601-1610.

Reference

1. J. P. Perdew, K. Burke, M. Ernzerhof, Phys. Rev. Lett. 1996, 77, 3865.
2. G. Kresse, D. Joubert, Phys. Rev. B 1999, 59, 1758.
3. J.P. Perdew, K. Burke, M. Ernzerhof, Phy. Rev. Lett. 77 (1996) 3865.
4. S. Grimme, J. Antony, S. Ehrlich, and S. Krieg, J. Chem. Phys. 132, 154104 (2010).
5. H. J. Monkhorst, J. D. Pack, Phys. Rev. B 1976, 13, 5188.
6. Z. Zhang, J. Sun, F. Wang and L. Dai, Angewandte Chemie International Edition, 2018, 57, 9038-9043.